AMERICAN SOCIETY FOR MICROBIOLOGY | Journal of Bacteriology®

RESEARCH ARTICLE

Characterization of RelA in *Acinetobacter baumannii*

María Pérez-Varela,[a,c] Aimee R. P. Tierney,[a,c] Ju-Sim Kim,[d] Andrés Vázquez-Torres,[d,e] Philip Rather[a,b,c]

[a]Department of Microbiology and Immunology, Emory University School of Medicine, Atlanta, Georgia, USA
[b]Research Service, Veterans Affairs Medical Center, Decatur, Georgia, USA
[c]Emory Antibiotic Resistance Center, Emory University School of Medicine, Atlanta, Georgia, USA
[d]Department of Immunology and Microbiology, University of Colorado School of Medicine, Aurora, Colorado, USA
[e]Veterans Affairs Eastern Colorado Health Care System, Denver, Colorado, USA

ABSTRACT In response to nutrient depletion, the RelA and SpoT proteins generate the signaling molecule (p)ppGpp, which then controls a number of downstream effectors to modulate cell physiology. In *Acinetobacter baumannii* strain AB5075, a *relA* ortholog (*ABUW_3302*) was identified by a transposon insertion that conferred an unusual colony phenotype. An in-frame deletion in *relA* (Δ*relA*) failed to produce detectable levels of ppGpp when amino acid starvation was induced with serine hydroxamate. The Δ*relA* mutant was blocked from switching from the virulent opaque colony variant (VIR-O) to the avirulent translucent colony variant (AV-T), but the rate of AV-T to VIR-O switching was unchanged. In addition, the Δ*relA* mutation resulted in a pronounced hypermotile phenotype on 0.35% agar plates. This hypermotility was dependent on the activation of a LysR regulator ABUW_1132, which was required for expression of AbaR, a LuxR family quorum-sensing regulator. In the Δ*relA* mutant, ABUW_1132 was also required for the increased expression of an operon composed of the *ABUW_3766-ABUW_3773* genes required for production of the surfactant-like lipopeptide acinetin 505. Additional phenotypes identified in the Δ*relA* mutant included (i) cell elongation at high density, (ii) reduced formation of persister cells tolerant to colistin and rifampin, and (iii) decreased virulence in a *Galleria mellonella* model.

IMPORTANCE *Acinetobacter baumannii* is a pathogen of worldwide importance. Due to the increasing prevalence of antibiotic resistance, these infections are becoming increasingly difficult to treat. New therapies are required to combat multidrug-resistant isolates. The role of RelA in *A. baumannii* is largely unknown. This study demonstrates that like in other bacteria, RelA controls a variety of functions, including virulence. Strategies to inhibit the activity of RelA and the resulting production of ppGpp could inhibit virulence and may represent a new therapeutic approach.

KEYWORDS *Acinetobacter*, stringent response, quorum sensing, motility

Acinetobacter baumannii is a nosocomial pathogen responsible for a variety of human infections (1–5). The incidence of these infections is increasing worldwide, and the inability to effectively treat these infections with antibiotics is a worrisome development, as recently emphasized by both the U.S. Centers for Disease Control and Prevention and the World Health Organization (6–9). Furthermore, *A. baumannii* infections can be seen in the community and can cause a severe rapidly fatal disease (10, 11).

A. baumannii strain AB5075 and many clinical isolates can switch between two cell types, those that form opaque colonies on 0.5× Luria-Bertani (LB) agar plates when viewed by oblique lighting and those that form translucent colonies (12). These two cell types exhibit marked differences in virulence in both *Galleria mellonella* and mouse

Citation Pérez-Varela M, Tierney ARP, Kim J-S, Vázquez-Torres A, Rather P. 2020. Characterization of RelA in *Acinetobacter baumannii*. J Bacteriol 202:e00045-20. https://doi.org/10.1128/JB.00045-20.

Editor George O'Toole, Geisel School of Medicine at Dartmouth

Copyright © 2020 American Society for Microbiology. All Rights Reserved.

Address correspondence to Philip Rather, prather@emory.edu.

Received 22 January 2020
Accepted 26 March 2020
Accepted manuscript posted online 30 March 2020
Published 27 May 2020

lung models of infection, where the opaque form is virulent (VIR-O) and the translucent form is avirulent (AV-T) (12, 13). Several regulatory genes can influence the rate of VIR-O to AV-T switching. For example, mutations in *arpAB* encoding an RND-type efflux system decrease the rate of switching, and mutations in orthologs of the EnvZ/OmpR two-component system increase the rate of VIR-O to AV-T switching (14, 15). In addition, overexpression of a TetR-type transcriptional regulator, ABUW_1645, can drive cells from the VIR-O to the AV-T state. However, a null allele in *ABUW_1645* had no effect on VIR-O to AV-T switching (13).

Bacteria respond to starvation for carbon, fatty acid, phosphate, iron, and amino acids and other stress responses by inducing synthesis of the alarmone molecule (p)ppGpp via the RelA or SpoT protein, reviewed in references 16 to 20. RelA and SpoT comprise the RSH superfamily, in which RelA synthesizes (p)ppGpp using ATP and GDP/GTP and SpoT has both weak synthetase activity and strong hydrolase (ppGpp degrading) activity. The effect of ppGpp accumulation in cells is multifactorial. Global transcription is reprogrammed utilizing ppGpp together with the DksA protein to alter the activity of RNA polymerase (RNAP), resulting in both decreased and increased transcription at various promoters (16, 19, 21, 22). A second mechanism for transcriptional reprogramming by ppGpp involves decreasing the affinity of σ^{70} for RNAP and allowing other sigma factors to bind (23). RelA and the resulting production of ppGpp impacts additional cellular functions, including growth rate, translation, and DNA replication (16, 20). A requirement for ppGpp in bacterial virulence has been demonstrated in a wide variety of Gram-negative bacteria, including *Pseudomonas aeruginosa*, *Legionella pneumophila*, *Burkholderia pseudomallei*, *Francisella novicida*, *Vibrio cholerae*, *Yersinia pestis*, *Salmonella enterica*, and *Escherichia coli* (24–32). The role of RelA and ppGpp in the formation of antibiotic-tolerant persister cells has also been described (33–38). Reviews on this subject highlight the multiple roles attributed to RelA, including examples in Gram-positive bacteria (16, 39, 40).

In *A. baumannii*, the role of RelA is largely unknown. A screen for transposon insertions that resulted in sensitivity to ascites fluid or human serum identified *relA*, but no additional characterization was reported (41, 42). A recent study demonstrated a role for RelA in the regulation of efflux genes, such as *adeB* and *adeJ* (43). In this study, we report a transposon insertion in *relA* that was initially identified by the resulting change in colony morphology. Further characterization of an in-frame *relA* deletion revealed that a number of phenotypes were impacted by the mutation, including (i) loss of ppGpp synthesis, (ii) loss of switching from the VIR-O to the AV-T variant, (iii) increased surface motility, and (iv) elongated cell morphology at high density. Furthermore, like in many other bacteria, the loss of *relA* decreased virulence when assessed in a *Galleria mellonella* model. This study reveals for the first time the multiple roles for RelA in the physiology of *A. baumannii*.

RESULTS

Identification of an *A. baumannii relA* ortholog. *A. baumannii* strain AB5075 can rapidly switch between two cell types, virulent and avirulent, that are distinguished by their opaque (VIR-O) or translucent (AV-T) colony phenotypes when viewed with a light source that illuminates the colonies from below (oblique lighting) (12, 13). In the course of screening a transposon insertion library (EZ-Tn*5* <Tet-1>) in the avirulent translucent (AV-T) variant of AB5075, a colony with an unusual phenotype was observed that exhibited a metallic sheen and an irregular colony surface when viewed by oblique lighting. This colony phenotype was similar to that of mutants we had previously observed, where cells were highly filamentous (44). When this colony was restreaked, it gave rise to a second colony phenotype that was larger and flat with irregular edges. To identify this mutation, the transposon insertion was cloned out along with flanking DNA, and the insertion site was determined to be within the *ABUW_3302* gene. The protein encoded by *ABUW_3302* exhibited 40% identity and 62% amino acid similarity to the *E. coli* RelA protein. RelA functions as a ppGpp synthetase that generates the secondary messenger molecule (p)ppGpp in response to nutrient starvation and other

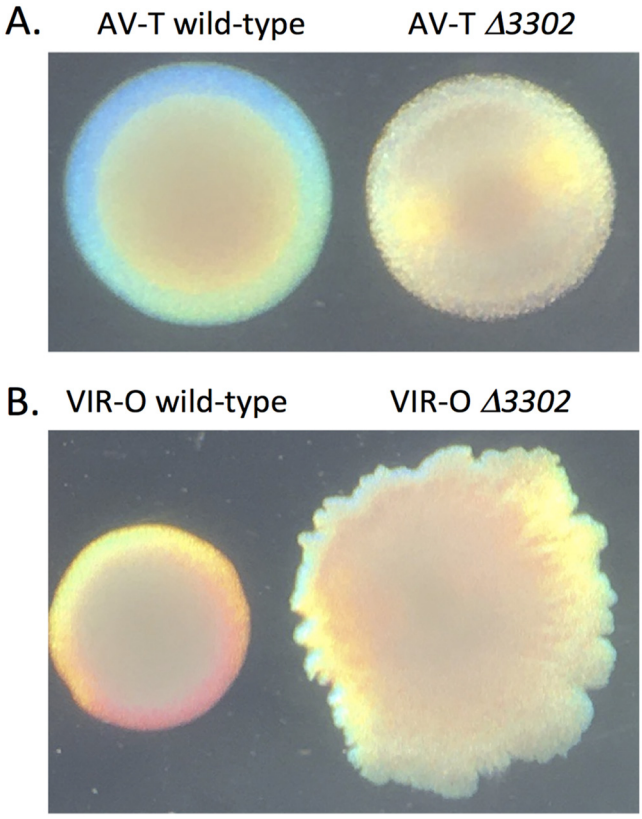

FIG 1 Colony morphology of wild-type and Δ*3302* mutants. (A) Colonies of the wild-type AV-T and the isogenic AV-T Δ*3302* mutant are shown after 24 h of growth on a 0.5× LB agar plate. (B) Colonies of the VIR-O wild type and the isogenic VIR-O Δ*3302* mutant are shown after 24 h of growth on a 0.5× LB agar plate. Because of the larger size of the VIR-O Δ*3302* colony, the relative picture size in panel B is approximately 50% smaller than in panel A.

stressors (19, 45). To confirm that the insertion in *ABUW_3302* was responsible for the observed colony phenotypes, a nonpolar in-frame deletion in *ABUW_3302* was constructed in both the VIR-O and AV-T variants. The AV-T Δ*ABUW_3302* mutant exhibited the same unusual colony phenotype as the original transposon insertion, and this phenotype is shown compared to a wild-type AV-T colony (Fig. 1A). In addition, the AV-T Δ*ABUW_3302* mutant was capable of switching at high frequency (~5% to 10%) to cells that now formed large flat colonies with irregular borders that were identical in appearance to colonies observed arising in the original AV-T transposon mutant. Moreover, these colonies were identical in appearance to the VIR-O Δ*ABUW_3302* mutant, confirming that these represented VIR-O variants (Fig. 1B). Taken together, these data indicate that the Δ*ABUW_3302* mutation significantly alters colony morphology in both the VIR-O and AV-T variants.

A deletion of *ABUW_3302* blocks the VIR-O to AV-T switch. As noted above, the AV-T Δ*ABUW_3302* mutant gave rise at high frequency to colonies identical in appearance to the VIR-O Δ*ABUW_3302* mutant. However, the VIR-O Δ*ABUW_3302* mutant did not give rise to colonies of the AV-T morphology when restreaked. To determine if the rate of VIR-O to AV-T switching was reduced by the Δ*ABUW_3302* mutation, the frequency of switching in 24-h colonies was determined (Table 1). While the rate of VIR-O to AV-T was measured at 6.6% in wild-type cells, we could not detect any AV-T colonies arising from the VIR-O mutant in the Δ*ABUW_3302* mutant background. The lower limit of detection in these switching assays is estimated to be $1/10^5$ to $1/10^6$ cells, making the decrease in switching at least 5,000-fold. Interestingly, when the rate of AV-T to VIR-O switching was determined, the levels were similar in wild-type cells and the Δ*ABUW_3302* mutant, 7.5% ± 1.7% and 10.9% ± 6.8%, respec-

TABLE 1 Analysis of switching frequency between VIR-O and AV-T variants

Strain or genotype	VIR-O to AV-T (%)	AV-T to VIR-O (%)
Wild type	6.6 ± 2.9	7.5 ± 1.7
Δ*ABUW_3302*	None detected	10.9 ± 6.8
Δ*ABUW_3302*/Tn*7*::*ABUW_3302*	20.5 ± 8.6	Not determined

tively. To determine whether providing the Δ*ABUW_3302* gene in *trans* could complement the Δ*ABUW_3302* mutation, an isopropyl-β-D-thiogalactopyranoside (IPTG)-inducible copy of Δ*ABUW_3302* was introduced into the chromosome at the *glmS* site on a Tn*7* derivative. In the presence of 2 mM IPTG, the Δ*ABUW_3302*/Tn*7*::*ABUW_3302* cells now exhibited a normal colony morphology, and the rate of VIR-O to AV-T switching was restored to 20.5% ± 8.6%.

The *ABUW_3302* gene encodes a RelA ortholog. To determine whether the *ABUW_3302* gene encoded a ppGpp synthetase, the production of ppGpp was examined by thin-layer chromatography in the presence or absence of serine hydroxamate, an inducer of the RelA-dependent stringent response. In wild-type cells, the presence of serine hydroxamate induced the production of ppGpp. However, the Δ*relA* mutant was unable to produce ppGpp, confirming that it functioned as a ppGpp synthetase (Fig. 2). Based on this result and the amino acid similarity of the *ABUW_3302* gene product to those of the RelA proteins of other bacteria, the *ABUW_3302* gene will be referred to here as *relA*.

The Δ*relA* mutation results in cell elongation at high density. Cells of the wild-type VIR-O and AV-T variants and the corresponding isogenic Δ*relA* mutants were examined by phase-contrast microscopy at mid-log phase and at early stationary phase. In mid-log-phase cultures, both wild-type and Δ*relA* cells from either VIR-O or AV-T backgrounds exhibited similar morphologies (Fig. 3). However, at high cell density, the Δ*relA* mutation in both the VIR-O and AV-T backgrounds resulted in elongated cells relative to the wild type, which was restored by a wild-type copy of *relA* (Fig. 3).

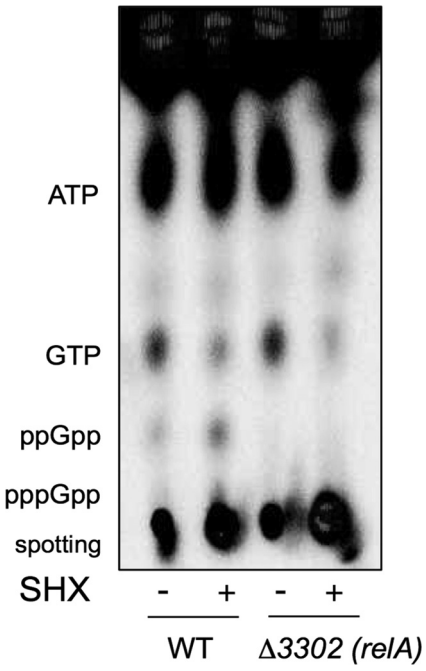

FIG 2 TLC autoradiogram of ^{32}P-labeled nucleotides from the AB5075 VIR-O wild type (WT) and the Δ*ABUW_3302* (*relA*) mutant after exposure to 0.4 mg/ml serine hydroxamate (SHX) for 5 min. The autoradiogram shown is representative of three independent experiments.

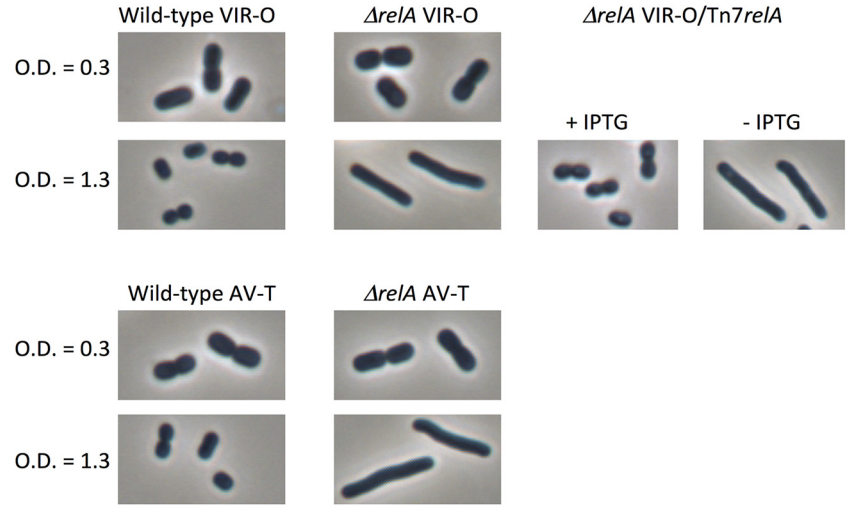

FIG 3 Cell morphology at low and high cell densities. Cells were grown in LB and examined microscopically at early log phase (OD_{600} of 0.3) or at high density (OD_{600} of 1.3).

The Δ*relA* mutation results in a hypermotile phenotype. Based on the flat, irregular, and spreading colonies formed by the VIR-O Δ*relA* mutant on 0.5× LB agar plates, we predicted that cells would be hypermotile, as a similar colony phenotype and hypermotility was previously observed in an *arpB* mutant (14). When motility was measured on 0.35% agar plates, the VIR-O Δ*relA* mutant was indeed hypermotile relative to wild-type cells (Fig. 4A). However, this increase in motility was specific to the VIR-O form. When the AV-T Δ*relA* mutant was tested for motility, it was similar to wild-type AV-T cells (data not shown). Introduction of the wild-type *relA* gene under the control of an IPTG-inducible *tac* promoter in single copy (Tn*7*) into the VIR-O Δ*relA* mutant reduced motility back to wild-type levels when *relA* expression was induced with IPTG (Fig. 4A).

RelA represses quorum sensing. Previous studies have indicated that surface motility in *A. baumannii* and *Acinetobacter nosocomialis* is dependent on a number of factors, including (i) production of the quorum-sensing signal 3-OH C_{12}-homoserine lactone (HSL) mediated by the AbaI autoinducer synthase, which is activated by the AbaR transcriptional regulator (46), (ii) 1, 3-diaminopropane produced by the combined activity of the Dat and Ddc proteins (47), (iii) acinetin 505, a surfactant-like molecule produced by proteins encoded by a large operon, *ABUW_3766-ABUW_3773* (46, 48), and (iv) loss of the histone-like protein H-NS (49). To determine if the Δ*relA* mutation altered the expression of genes encoding these motility-related factors, we used quantitative real-time PCR (qRT-PCR) to measure expression of these genes in wild-type VIR-O and isogenic Δ*relA* backgrounds. Expression of *abaI*, *abaR*, and *ABUW_3770*, a representative gene in the *ABUW_3766-ABUW_3773* operon, were upregulated 3.9-fold, 41.3-fold, and 55.6-fold, respectively, in the Δ*relA* mutant (Table 2). In contrast, expression of *ABUW_1109* (*dat*) and *ABUW_3609* (*hns*) was not significantly altered in the Δ*relA* mutant (Table 2). Introduction of a wild-type copy of *relA* on a Tn*7* derivative into the Δ*relA* mutant reduced the levels of *abaI*, *abaR*, and *ABUW_3770* expression back to wild-type levels (Table 2).

Next, to evaluate if hypermotility in the Δ*relA* mutant was dependent on overexpression of the *abaI*, *abaR*, or *ABUW_3770* gene, *abaI*::*T26*, *abaR*::*T26*, and *ABUW_3770*::*T26* mutations were individually introduced into the Δ*relA* background, and all these mutations resulted in loss of the hypermotile phenotype (Fig. 4A).

RelA controls motility and quorum sensing via ABUW_1132, a LysR-type regulator. In the course of screening an *A. baumannii* plasmid library for a separate study, a transformant was identified that produced large flat colonies with irregular edges on 0.5× LB agar plates. This phenotype was very similar to that seen in the Δ*relA* mutant

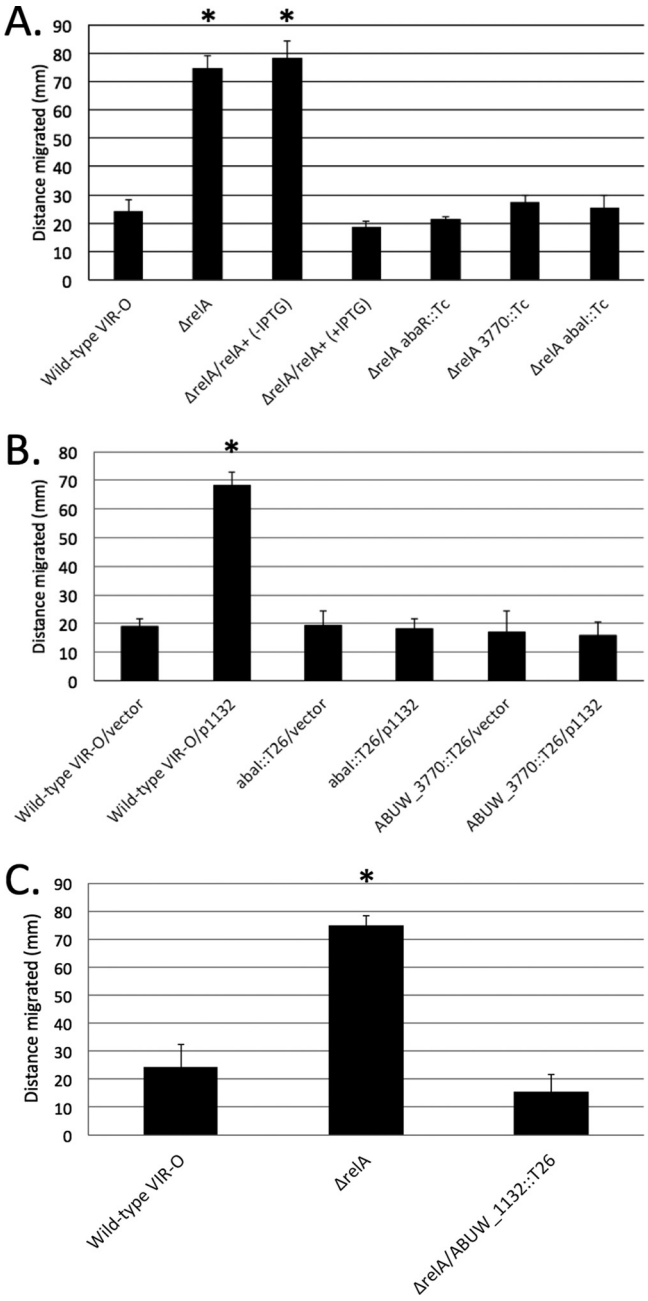

FIG 4 Surface motility of *A. baumannii* strains. Cultures of strains to be tested were grown to an optical density of 0.5, and a 1-μl aliquot was placed on the surface of a 0.35% Eiken agar plate. Plates were incubated at 37°C for 8 h. The reported values represent the averages from 6 measurements per strain, 2 from three independent experiments. *, $P < 0.05$ versus wild-type control determined by Student's *t* test.

and suggested a hypermotile phenotype. The only functional gene within this insert was *ABUW_1132*, encoding a predicted LysR-type transcriptional regulator. To verify that motility was increased in this transformant, surface motility was examined on 0.35% Eiken agar plates. The presence of *ABUW_1132* in multicopy (p1132) resulted in a 3.8-fold increase in motility compared to that of the vector control (Fig. 4B). In a manner similar to that seen in the Δ*relA* mutant, the hypermotile phenotype resulting from *ABUW_1132* overexpression was lost in *abaI*::*T26* and *ABUW_3770*::*T26* mutants, indicating that a functional quorum-sensing pathway and acinetin 505 synthesis were required (Fig. 4B).

TABLE 2 Real-time qRT-PCR analysis of gene expression

Strain or genotype	Relative expression of[a]:					
	abaI	*abaR*	*ABUW_3770*	*dat* (*ABUW_1109*)	*hns* (*ABUW_3609*)	*ABUW_1132*
Wild type	1	1	1	1	1	1
Δ*relA*	3.9 ± 1.3	41.3 ± 10.4[b]	55.6 ± 17.1[b]	1.7 ± 0.3	1.5 ± 0.3	14.2 ± 1.0[b]
Δ*relA/ABUW_1132*::*T26*	1.7 ± 0.7	7.9 ± 3.0[c]	0.9 ± 0.3[c]			
Δ*relA* Tn*7relA*[d]	0.8 ± 0.1	1.2 ± 0.2	0.9 ± 0.2			0.8 ± 0.1

[a]Values represent the means from three biological replicates with standard errors. Values for each strain were calculated using the $2^{-\Delta\Delta CT}$ method with *clpX* as an internal control.
[b]$P < 0.05$ versus wild type.
[c]$P < 0.05$ versus Δ*relA*.
[d]Cells with Tn*7relA* were grown with 5 mM IPTG.

Since the motility phenotype resulting from *ABUW_1132* overexpression and that of the Δ*relA* mutant were similar, two additional experiments were conducted to determine if the increased motility in the Δ*relA* mutant was due to *ABUW_1132* overexpression. First, qRT-PCR analysis of *ABUW_1132* mRNA levels in a wild-type VIR-O and the isogenic Δ*relA* mutant verified that expression of *ABUW_1132* was increased 14.2 ± 1.0-fold in the Δ*relA* mutant (Table 2). The increased *ABUW_1132* expression was brought back to wild-type levels in the Δ*relA* mutant containing a wild-type copy of *relA* (Tn*7relA*). Next, to determine if the increased *ABUW_1132* expression in the Δ*relA* mutant was responsible for activation of the downstream *abaI*, *abaR*, and *ABUW_3770* genes, the expression of these genes was examined by qRT-PCR in the Δ*relA* mutant and in a Δ*relA ABUW_1132*::*T26* double mutant. The increased expression of *abaI*, *abaR*, and *ABUW_3770* in the Δ*relA* mutant was now lost or significantly reduced in the Δ*relA ABUW_1132*::*T26* double mutant (Table 2). In addition, the hypermotile phenotype observed in the *relA* mutant was now lost in the Δ*relA ABUW_1132*::*T26* double mutant (Fig. 4C).

Role of RelA in persister cell formation. Strain AB5075 is highly resistant to most antibiotics and only exhibits sensitivity to a limited number of bactericidal antibiotics, such as colistin and rifampin. The MICs for colistin and rifampin were similar in both the wild-type VIR-O and the Δ*relA* mutant, with the rifampin MIC at 2 μg/ml and the colistin MIC at 0.38 μg/ml. Next, to determine if RelA contributed to the development of persister cells tolerant to high levels of antibiotic, cell survival was assayed after 1 h of exposure to 50× the MIC for colistin or 80× the MIC for rifampin. For wild-type VIR-O with rifampin, the percentage of surviving VIR-O cells was 22.3% ± 10.9%, and for the Δ*relA* mutant it was 6.3% ± 5.9%, representing a 3.5-fold decrease. For wild-type VIR-O, the percentage of cells surviving colistin was 7.9% ± 1.9%. For the Δ*relA* mutant, the percentage of surviving cells was 1.7% ± 0.5%, a 4.6-fold decrease ($P < 0.05$ versus the wild type).

RelA is required for virulence in *Galleria mellonella*. To investigate the role of RelA in virulence, larvae of the *Galleria mellonella* moth were utilized. Larvae ($n = 30$/strain) were infected with 9×10^5 cells of the wild-type VIR-O or isogenic Δ*relA* mutant, and survival was monitored over a 5-day period. The Δ*relA* mutant exhibited reduced virulence, as indicated by the increased overall survival after 5 days relative to that of larvae infected with wild-type VIR-O cells ($P < 0.001$) (Fig. 5). The reduced virulence of the Δ*relA* mutant was restored when a copy of *relA* (Tn*7relA*) was introduced (Fig. 5).

DISCUSSION

In this study, we have identified and characterized a RelA ortholog in *A. baumannii* and demonstrated that it regulates multiple cellular functions. Our initial identification of the Δ*relA* mutation resulted from a transposon insertion in the avirulent translucent (AV-T) colony variant that gave an unusual colony phenotype when viewed by oblique lighting under a dissecting microscope. This phenotype was likely the result of elongated cells that changed the colony appearance. This finding is consistent with previous studies that have shown that *relA* mutations and the resulting loss of ppGpp

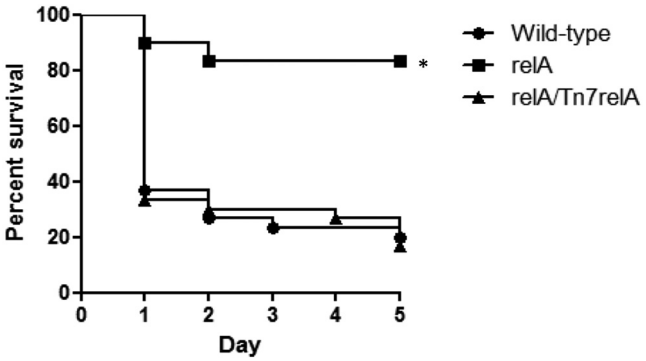

FIG 5 Virulence assays using *Galleria mellonella*. Larvae weighing between 200 and 250 mg were injected with 9×10^5 cells of the indicated strains. Larvae were monitored daily for survival for a period of 5 days. The reported values represent the averages from 30 larvae from a total of three independent experiments where 10 larvae/strain were used. *, $P < 0.001$ by the Mantel-Cox test.

can also result in cell elongation (50–52). Additional changes in colony morphology due to loss of *relA* were evident in virulent opaque (VIR-O) cells, where colonies exhibited a spreading morphology on 0.5× agar plates, a phenotype consistent with increased surface motility.

The Δ*relA* mutation in a VIR-O background resulted in a 3-fold increase in surface motility (Fig. 4A). This increased motility was dependent on the LysR-type transcriptional regulator ABUW_1132, AbaI (autoinducer synthase), AbaR (LuxR-type regulator), and ABUW_3770. Previous studies in *A. nosocomialis* M2 have shown that *abaI*, encoding an autoinducer synthase responsible for the production of 3-OH C_{12}-HSL, was required for surface motility (46). In addition, the AbaI-dependent quorum-sensing pathway in *A. nosocomialis* was responsible for activating a large operon highly similar to *A1S_0112-A1S_0119* in *A. baumannii* strain ATCC 17978 and to *ABUW_3766-ABUW_3773* in *A. baumannii* AB5075 (46). Recent work has shown the *A1S_0112-A1S_0119* gene products direct the production of acinetin 505, a surfactant-like lipopeptide (48). In the Δ*relA* mutant, expression of *abaR* and *ABUW_3770* (a representative gene for the *ABUW_3766-ABUW_3773* operon) were upregulated 41-fold and 56-fold, respectively. This suggests the following mechanism to explain the hypermotile phenotype in the Δ*relA* mutant (Fig. 6). First, loss of *relA* increases ABUW_1132 expression, which directly or indirectly activates AbaR. In turn, together with 3-OH C_{12}-HSL, AbaR then activates the *ABUW_3766-ABUW_3773* operon, which increases acinetin 505 production and aids cell motility by its surfactant-like qualities. However, the loss of *relA* may also increase *abaR* expression in a manner independent of ABUW_1132, as the levels of expression in the *relA ABUW_1132*::*T26* double mutant are still elevated above wild-type levels (Table 2). Interestingly, the effect of RelA on the quorum-sensing

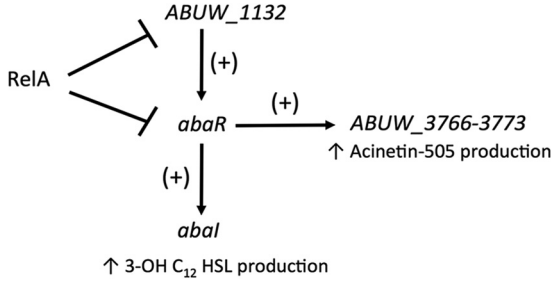

FIG 6 A model for the RelA-dependent control of downstream pathways. RelA is predicted to act as a negative regulator of both the LysR-type regulator ABUW_1132 and the LuxR-type regulator AbaR. ABUW_1132 then activates the *abaR* gene and, together with 3-OH C_{12}-HSL, AbaR then activates the *abaI* gene and the *ABUW_3766-ABUW_3773* operon.

response in *A. baumannii* differs from that seen in *Pseudomonas aeruginosa*, where quorum sensing is activated in a RelA-dependent manner (53).

The Δ*relA* mutation completely blocked the ability of *A. baumannii* AB5075 to switch from the virulent opaque form (VIR-O) to the avirulent translucent form (AV-T). This phenotype was fully complemented by expressing a single copy of the *relA* gene from an IPTG-inducible promoter. Interestingly, the reciprocal AV-T to VIR-O switch was unaffected by the Δ*relA* mutation. A similar effect on switching was also observed in *arpAB* mutants, where switching was decreased in the VIR-O to AV-T direction only (14). This adds support to the hypothesis that separate pathways can control the directionality of this virulence switch. Since *arpAB* mutants exhibited a defect in switching, we determined if the Δ*relA* mutation decreased expression of these genes, but similar levels were observed in the wild type and the Δ*relA* mutant (M. Perez-Varela and P. Rather, unpublished data). Despite being locked in the virulent opaque form, the Δ*relA* mutant exhibited a significant decrease in virulence when tested in a *Galleria mellonella* model. Reduced virulence is a common phenotype resulting from loss of RelA in other bacteria (24–32). The contribution of decreased switching from the VIR-O to the AV-T form to the overall levels of virulence *in vivo* are likely to be minimal, as the majority of cells will be in the VIR-O form either way. Therefore, in the absence of other genetic changes, simply locking a strain in the VIR-O state may not increase virulence. The reduced virulence of the Δ*relA* mutant is likely due to global pleiotropic changes that negatively impact virulence.

The mechanism by which the Δ*relA* mutation results in loss of switching from the VIR-O to AV-T state is under investigation. However, a Δ*relA ABUW_1132* double mutant did not exhibit restored switching, indicating that the RelA-mediated upregulation of *ABUW_1132* was not involved (Perez-Varela and Rather, unpublished). It is possible that ppGpp directly influences the activity of a transcriptional regulatory protein in a manner similar to that seen with SlyA in *S. enterica* serovar Typhimurium and PigR in *Francisella tularensis* (54, 55). Alternatively, the loss of switching may result from a more general mechanism due to the global changes in gene expression brought about by reprogramming RNA polymerase. We are currently investigating these possibilities by conducting suppressor screens to identify mutations or high-copy-number suppressors that restore VIR-O to AV-T switching in the Δ*relA* mutant. Additionally, a SpoT ortholog (ABUW_0309) is present in *A. baumannii*, and its role in *A. baumannii* is under investigation.

MATERIALS AND METHODS

Strains and growth conditions. *A. baumannii* AB5075 was grown in modified Luria-Bertani (LB) broth (10 g tryptone, 5 g yeast extract, 5 g NaCl per liter) at 37°C with shaking at 270 rpm. LB agar plates were prepared either full strength (1× LB), using 10 g tryptone, 5 g yeast extract, and 5 g NaCl per liter and 1.5% agar, or half strength (0.5× LB), using 5 g tryptone, 2.5 g yeast extract, and 2.5 g NaCl per liter and 0.8% agar. To prepare competent AB5075 AV-T, cells were grown to an optical density at 600 nm (OD_{600}) of 0.8, pelleted by centrifugation, and washed twice with 1 ml of ice-cold 10% glycerol. Competent cells were resuspended in 70 μl of ice-cold 10% glycerol per electroporation. Following electroporation, cells were resuspended in 1 ml of LB broth and recovered by stationary incubation at 37°C for 30 min followed by 30 min of incubation at 270 rpm. Isopropyl-β-D-thiogalactopyranoside (IPTG) was added at a final concentration of 2 μM to media.

Measurement of (p)ppGpp pools. Nucleotides were measured as described previously (56, 57). *A. baumannii* cells were grown in morpholinepropanesulfonic acid (MOPS) minimal medium supplemented with 0.4% D-glucose, 40 μg/ml of each amino acid except serine, and 0.4 mM phosphate. MOPS minimal medium consisted of 40 mM MOPS buffer, 4 mM tricine, 0.4% D-glucose, 40 μg/ml of each amino acid except serine, 2 mM K_2HPO_4, 10 μM $FeSO_4{\cdot}7H_2O$, 9.5 mM NH_4Cl, 276 μM K_2SO_4, 500 nM $CaCl_2$, 50 mM NaCl, 525 μM $MgCl_2$, 2.9 nM $(NH_4)_6Mo_7O_{24}{\cdot}4H_2O$, 400 nM H_3BO_3, 30 nM $CoCl_2$, 9.6 nM $CuSO_4$, 80.8 nM $MnCl_2$, and 9.74 nM $ZnSO_4$ (pH 7.2) (58). Logarithmically grown bacterial cultures (OD_{600} of 0.25) were labeled with 10 μCi/ml of [^{32}P]phosphorous (PerkinElmer, Waltham, MA) for approximately 1.5 doubling times (60 min). Cells were treated with 0.4 mg/ml serine hydroxamate for 5 min before 0.4 ml of ice-cold 50% formic acid was added to the cultures. Samples incubated on ice for at least 20 min were centrifuged at 13,000 rpm for 5 min. Five microliters of formic acid extracts was spotted along the bottom of polyethyleneimine-cellulose thin-layer chromatography (TLC) plates (20 cm by 20 cm; Millipore, Billerica, MA), and air-dried plates were separated with a 1.25 M KH_2PO_4 (pH 3.4) solvent system in a TLC chamber for 1 h. TLC autoradiograms were visualized using a phosphorimager (Bio-Rad, Hercules, CA).

Transposon mutagenesis. The AB5075 AV-T variant was mutagenized with EZ-Tn*5* <Tet-1> (Lucigen) per the manufacturer's instructions. The transposon solution (0.5 μl transposon, 0.5 μl transposase, 1.5 μl 10% glycerol) was incubated at 37°C for 1 h prior to electroporation into competent AB5075 AV-T cells. Electroporations were performed in Bio-Rad Gene Pulser 0.2-cm-gap cuvettes with a MicroPulser electroporator (Bio-Rad, Hercules, CA). Cells were plated on LB agar plates with tetracycline and incubated at 37°C for 24 h. Plates were inspected using a dissecting microscope with oblique lighting.

Identification of the EZ-Tn*5* <Tet-1> insertion site. To identify the insertion site of the EZ-Tn*5* <Tet-1> insertion, total genomic DNA from the mutant was partially digested with Sau3A, and fragments in the 2- to 4-kb range were gel purified, ligated into the BamHI site of pBC SK(−), and electroporated into EC100D competent cells (Lucigen, Middleton, WI). Cells were plated on LB agar plates containing 10 μg/ml tetracycline and incubated overnight at 37°C. To confirm that the insertions were present, plasmid DNA was purified from Tet^r colonies using the QIAprep Spin Miniprep kit (Qiagen, Hilden, Germany) prior to digestion with XbaI. Plasmids containing insertions were sequenced with primers FP1 and RP1 provided by the EZ-Tn*5* <Tet-1> insertion kit (Lucigen, Middleton, WI).

Microscopy. Cells were grown in LB to either mid-log phase (OD_{600} of 0.3) or to early stationary phase (OD_{600} of 1.3). Cells at mid-log phase were concentrated 10-fold prior to phase-contrast microscopy at ×1,000 magnification under an oil immersion lens.

Construction of an in-frame deletion in *relA*. To create an in-frame deletion mutant, a fragment upstream of the *relA* gene (RelA Up) which contains the first few codons of *relA* and flanking DNA was PCR amplified using primers Up-1 (5′-AAAAAGGATCCGCTTGAGCCTTTTTCTCACC-3′) and Up-2 (5′-GCAC GACGCATGATTCAAG-3′). A second fragment downstream of *relA* (RelA Down) containing the last few *relA* codons and flanking DNA was PCR amplified using primers Down-1 (5′-CTGTTCACGTACTGTGA CCAT-3′) and Down-2 (5′-AAAAAGGATCCTAAGCGCCATCCAACTTTAGT-3′). Primers Up-2 and Down-1 were previously phosphorylated using T4 polynucleotide kinase (New England BioLabs, Beverly, MA). RelA Up and RelA Down were ligated for 2 h, run on a 0.8% Tris-acetate-EDTA (TAE) gel, and the gel section corresponding to the size of the combined fragments was gel purified. The fragment was PCR amplified using primers Up-1 and Down-2 to create the Δ*relA* fragment, which was digested and ligated into the BamHI site of pEX18Tc. The ligation was transformed into EC100D cells and plated on LB plates containing tetracycline (10 μg/ml). Plasmid DNA was isolated from Tet^r colonies and digested to confirm the presence of pEX18Tc-Δ*relA* construct. pEX18Tc-Δ*relA* was electroporated and maintained in *E. coli* SM10 λpir. *E. coli* SM10 λpir pEX18Tc-Δ*relA* was conjugated to the VIR-O variant of AB5075, and an Amp^r Tet^r Suc^s AB5075 exconjugant was grown in LB broth at 37°C for 1.5 h at 250 rpm. Cells were plated on LB (without NaCl) containing 10% sucrose and incubated at room temperature. Sucrose-resistant colonies were screened via PCR using primers Up-1 and Down-2 to confirm the deletion of *relA*.

Construction of a *relA*-complemented strain. A wild-type copy of the *relA* gene with its native ribosome binding site was generated by PCR using the primers AGGAGAATGGTATGGTCACAGTACG and ACTCTCAACAATAAGTCCCCAG. This PCR-generated fragment was then cloned into the SmaI site of pUC18Tn7 LAC Apr (kindly provided by Ayush Kumar at the University of Manitoba) (59). A recombinant containing the *relA* gene in the correct orientation such that expression could be driven by the IPTG-inducible *tac* promoter was electroporated along with a plasmid containing the Tn*7* transposase (pTNS2) into the Δ*relA* mutant. A strain with the correct insertion of the Tn*7*/*relA* into the *glmS* region of the chromosome was verified by PCR. This strain was then grown in the presence of IPTG at the indicated concentrations for complementation experiments.

Moving T26 transposon insertions into new backgrounds. A recent study reported that chromosomal markers could be moved between *A. baumannii* strains by phage-mediated generalized transduction (60). Based on this study, we determined that insertions from the comprehensive insertion library constructed by Colin Manoil's group at the University of Washington could be moved between strains by the same procedure. Overnight saturated cultures containing a given transposon insertion were spun down, and 1 ml of supernatant was filter sterilized (0.22 μm) to generate a phage lysate. To transduce the recipient strain, 20 μl of a mid-log-phase culture was mixed with 20 μl of lysate and spotted on the surface of a well-dried LB plate to allow the spot to quickly soak into the agar. After incubation at 37°C for 4 h, cells were scraped from the plate, resuspended in 2 ml of LB broth, and plated on LB plus tetracycline (5 μg/ml). Colonies were screened by PCR for the correct insertion.

Plasmid p1132 construction. Plasmid pQF1266 is a derivative of pQF50 (61) and contains a hygromycin resistance cassette cloned into the ScaI site of the β-lactamase gene and an origin of replication from pWH1266. A partial Sau3A digest of AB5075 chromosomal DNA was performed, and fragments in the size range of 3 to 6 kb were cloned into the BamHI site of pQF1266 (62). This genomic library was used in a variety of genetic screens, and a recombinant plasmid that generated a hypermotile colony was designated p1132. The only complete gene within this plasmid was *ABUW_1132*.

Analysis of VIR-O and AV-T switching frequencies. Aliquots of AB5075 VIR-O and AV-T variants in the wild-type and Δ*relA* mutant backgrounds were serially diluted, plated on 0.5× LB plates, and incubated at 37°C for 24 h. Plates containing fewer than 50 colonies were used, and 6 well-isolated colonies from each strain were removed from the plate as agar plugs and resuspended in 2 ml LB broth. Serial dilutions of 10^{-4}, 10^{-5}, and 10^{-7} were plated on 0.5× LB plates and incubated at 37°C for 24 h. Plates were inspected under a dissecting microscope via indirect light, and VIR-O and AV-T variants were quantified.

Motility assays. Motility assays were carried out on Eiken agar motility plates consisted of 10 g tryptone, 5 g yeast extract, 5 g NaCl, and 3.5 g Eiken agar (Eiken Chemical Ltd., Tokyo, Japan) per liter. The plates were prepared the same day of the assay and they were allowed to dry for 30 min before use. Strains were inoculated in LB broth medium and grown at 37°C with shaking until an OD_{600} of 0.5 was

reached. A 1-μl aliquot of the corresponding strain culture was spotted onto the 0.35% Eiken agar motility plates, and the plates were incubated at 37°C for approximately 8 h, which was previously determined to be the time required for the Δ*relA* mutant strain to reach the plate border under experimental conditions. Wild-type and Δ*relA* mutant strains were compared on the same plates. Motility diameters were measured after the designated time, and statistical analysis was performed using Student's *t* test. The relative migration was calculated as the ratio of the motility diameter of the studied strain to that of the corresponding control strain in each case. All assays were conducted a minimum of two independent times.

***Galleria mellonella* infections.** *G. mellonella* larvae were purchased from Speedy Worm, Alexandria, MN. For larval infections, the wild-type VIR-O variant of AB5075 and isogenic Δ*relA* mutant cultures were grown in 2 ml of LB broth at 37°C with shaking to an optical density (OD_{600}) of approximately 0.5. Serial dilutions were prepared in LB with 20% glycerol and stored in aliquots at −80°C. For infections, 9×10^5 cells were injected in an 8-μl volume with IPTG (10 mM) into the last proleg of *G. mellonella* larvae weighing between 200 and 250 mg. Larvae were incubated in a petri plate at 37°C in a humidified incubator for up to 5 days. The number of dead larvae was evaluated at 24-h intervals; larvae were considered dead when they were dark brown to black and showed no movement in response to touch with a pipette tip. Injections of LB alone did not result in killing. For all experiments, the serial dilutions used were plated onto regular LB plates to determine CFU per milliliter for each bacterial strain. The reported data correspond to three independent experiments carried out with 10 larvae for each strain.

RNA extraction and quantitative real-time PCR. Cultures of wild-type VIR-O strain AB5075 and the Δ*relA* mutant were grown in 2 ml of LB broth at 37°C with shaking to an OD_{600} of approximately 1.500. The cultures were centrifuged, and the RNA was isolated using the MasterPure RNA isolation kit (Lucigen, Middleton, WI) according to the manufacturer's instructions. The samples were treated with Turbo DNA-free DNase (Ambion) to remove the contaminating DNA. The RNA concentration was determined using a NanoDrop ND-1000 spectrophotometer, and cDNA was obtained by using the iScript cDNA synthesis kit (Bio-Rad, Hercules, CA) with random primers. The reverse transcription reaction was performed as follows: 25°C for 5 min, 42°C for 45 min, and 85°C for 5 min. Diluted cDNA (1:10) was used as the template for experimental reactions. Specific oligonucleotides pairs for quantitative real-time PCR (qRT-PCR) to amplify approximately 150-bp fragments from each gene of study were generated by using the Primer-BLAST program (www.ncbi.nlm.nih.gov/tools/primer-blast/). Gene expression was determined using iQ SYBR green Supermix (Bio-Rad, Hercules, CA) on a CFX Connect cycler (Bio-Rad). Cycle conditions to amplify and quantify fragments were the following: 95°C for 3 min and then 95°C for 10 s, 55°C for 10 s, and 72°C for 20 s, repeated 40 times. Melt curve data were then collected to confirm the specificity of the oligonucleotide primer set. Data were generated from two independent RNA isolation and cDNA preparations and three replicates for each primer pair. The expression level of the target genes was standardized relative to the transcription level of the housekeeping gene *clpX* using the threshold cycle ($2^{-\Delta\Delta CT}$) method (63). The statistical significance of the observed differences was confirmed by the analysis of variance (ANOVA) test.

Persister cell assays. Wild-type and Δ*relA* cells were grown to an OD_{600} of 1.1 and incubated for 1 h at 37°C with either rifampin at a final concentration of 160 μg/ml or colistin at a final concentration of 20 μg/ml. Dilutions were then plated for CFU on LB agar plates.

ACKNOWLEDGMENTS

This work was supported by funding from the Department of Veterans Affairs (I01BX001725 and IK6BX004470) and NIH (R21AI142489 to P.N.R., and R01AI36520, R01AI05449 and VAI01BX002073 to A.V.T.).

We thank Ayush Kumar at the University of Manitoba for providing pUC18-miniTn*7*-Lac-Apra. We are grateful to Sarah Dayman, Marjan Farokhyfar, and Daniel Knight for help with strain and plasmid constructions.

REFERENCES

1. Gootz TD, Marra A. 2008. *Acinetobacter baumannii*: an emerging multidrug-resistant threat. Expert Rev Anti Infect Ther 6:309–325. https://doi.org/10.1586/14787210.6.3.309.
2. Joly-Guillou ML. 2005. Clinical impact and pathogenicity of *Acinetobacter*. Clin Microbiol Infect 11:868–873. https://doi.org/10.1111/j.1469-0691.2005.01227.x.
3. Peleg AY, Seifert H, Paterson DL. 2008. *Acinetobacter baumannii*: emergence of a successful pathogen. Clin Microbiol Rev 21:538–582. https://doi.org/10.1128/CMR.00058-07.
4. Visca P, Seifert H, Towner KJ. 2011. *Acinetobacter* infection–an emerging threat to human health. IUBMB Life 63:1048–1054. https://doi.org/10.1002/iub.534.
5. Wong D, Nielsen TB, Bonomo RA, Pantapalangkoor P, Luna B, Spellberg B. 2017. Clinical and pathophysiological overview of *Acinetobacter* infections: a century of challenges. Clin Microbiol Rev 30:409–447. https://doi.org/10.1128/CMR.00058-16.
6. Tacconelli E, Carrara E, Savoldi A, Harbarth S, Mendelson M, Monnet DL, Pulcini C, Kahlmeter G, Kluytmans J, Carmeli Y, Ouellette M, Outterson K, Patel J, Cavaleri M, Cox EM, Houchens CR, Grayson ML, Hansen P, Singh N, Theuretzbacher U, Magrini N, Aboderin AO, Al-Abri SS, Awang Jalil N, Benzonana N, Bhattacharya S, Brink AJ, Burkert FR, Cars O, Cornaglia G, Dyar OJ, Friedrich AW, Gales AC, Gandra S, Giske CG, Goff DA, Goossens H, Gottlieb T, Guzman Blanco M, Hryniewicz W, Kattula D, Jinks T, Kanj SS, Kerr L, Kieny M-P, Kim YS, Kozlov RS, Labarca J, Laxminarayan R, Leder K, et al. 2018. Discovery, research, and development of new antibiotics: the WHO priority list of antibiotic-resistant bacteria and tuberculosis. Lancet Infect Dis 18:318–327. https://doi.org/10.1016/S1473-3099(17)30753-3.
7. Sievert DM, Ricks P, Edwards JR, Schneider A, Patel J, Srinivasan A, Kallen A, Limbago B, Fridkin S, National Healthcare Safety Network (NHSN) Team and Participating NHSN Facilities. 2013. Antimicrobial-resistant pathogens associated with healthcare-associated infections: summary of

data reported to the National Healthcare Safety Network at the Centers for Disease Control and Prevention, 2009-2010. Infect Control Hosp Epidemiol 34:1–14. https://doi.org/10.1086/668770.
8. Dijkshoorn L, Nemec A, Seifert H. 2007. An increasing threat in hospitals: multidrug-resistant *Acinetobacter baumannii*. Nat Rev Microbiol 5:939–951. https://doi.org/10.1038/nrmicro1789.
9. Rice LB. 2006. Challenges in identifying new antimicrobial agents effective for treating infections with *Acinetobacter baumannii* and *Pseudomonas aeruginosa*. Clin Infect Dis 43:S100–S105. https://doi.org/10.1086/504487.
10. Telang NV, Satpute MG, Dhakephalkar PK, Niphadkar KB, Joshi SG. 2011. Fulminating septicemia due to persistent pan-resistant community-acquired metallo-beta-lactamase (IMP-1)-positive *Acinetobacter baumannii*. Indian J Pathol Microbiol 54:180–182. https://doi.org/10.4103/0377-4929.77397.
11. Lowman W, Kalk T, Menezes CN, John MA, Grobusch MP. 2008. A case of community-acquired *Acinetobacter baumannii* meningitis - has the threat moved beyond the hospital? J Med Microbiol 57:676–678. https://doi.org/10.1099/jmm.0.47781-0.
12. Tipton KA, Dimitrova D, Rather PN. 2015. Phase-variable control of multiple phenotypes in *Acinetobacter baumannii* strain AB5075. J Bacteriol 197:2593–2599. https://doi.org/10.1128/JB.00188-15.
13. Chin CY, Tipton KA, Farokhyfar M, Burd EM, Weiss DS, Rather PN. 2018. A high-frequency phenotypic switch links bacterial virulence and environmental survival in *Acinetobacter baumannii*. Nat Microbiol 3:563–569. https://doi.org/10.1038/s41564-018-0151-5.
14. Tipton KA, Farokhyfar M, Rather PN. 2017. Multiple roles for a novel RND-type efflux system in *Acinetobacter baumannii* AB5075. Microbiologyopen 6:e00418. https://doi.org/10.1002/mbo3.418.
15. Tipton KA, Rather PN. 2017. An ompR/envZ two-component system ortholog regulates phase variation, osmotic tolerance, motility, and virulence in *Acinetobacter baumannii* strain AB5075. J Bacteriol 199:e00705-16. https://doi.org/10.1128/jb.00705-16.
16. Potrykus K, Cashel M. 2008. (p)ppGpp: still magical? Annu Rev Microbiol 62:35–51. https://doi.org/10.1146/annurev.micro.62.081307.162903.
17. Irving SE, Corrigan RM. 2018. Triggering the stringent response: signals responsible for activating (p)ppGpp synthesis in bacteria. Microbiology 164:268–276. https://doi.org/10.1099/mic.0.000621.
18. Atkinson GC, Tenson T, Hauryliuk V. 2011. The RelA/SpoT homolog (RSH) superfamily: distribution and functional evolution of ppGpp synthetases and hydrolases across the tree of life. PLoS One 6:e23479. https://doi.org/10.1371/journal.pone.0023479.
19. Hauryliuk V, Atkinson GC, Murakami KS, Tenson T, Gerdes K. 2015. Recent functional insights into the role of (p)ppGpp in bacterial physiology. Nat Rev Microbiol 13:298–309. https://doi.org/10.1038/nrmicro3448.
20. Srivatsan A, Wang JD. 2008. Control of bacterial transcription, translation and replication by (p)ppGpp. Curr Opin Microbiol 11:100–105. https://doi.org/10.1016/j.mib.2008.02.001.
21. Paul BJ, Barker MM, Ross W, Schneider DA, Webb C, Foster JW, Gourse RL. 2004. DksA: a critical component of the transcription initiation machinery that potentiates the regulation of rRNA promoters by ppGpp and the initiating NTP. Cell 118:311–322. https://doi.org/10.1016/j.cell.2004.07.009.
22. Paul BJ, Berkmen MB, Gourse RL. 2005. DksA potentiates direct activation of amino acid promoters by ppGpp. Proc Natl Acad Sci U S A 102:7823–7828. https://doi.org/10.1073/pnas.0501170102.
23. Jishage M, Kvint K, Shingler V, Nystrom T. 2002. Regulation of sigma factor competition by the alarmone ppGpp. Genes Dev 16:1260–1270. https://doi.org/10.1101/gad.227902.
24. Erickson DL, Lines JL, Pesci EC, Venturi V, Storey DG. 2004. *Pseudomonas aeruginosa relA* contributes to virulence in *Drosophila melanogaster*. Infect Immun 72:5638–5645. https://doi.org/10.1128/IAI.72.10.5638-5645.2004.
25. Hammer BK, Swanson MS. 1999. Co-ordination of *Legionella pneumophila* virulence with entry into stationary phase by ppGpp. Mol Microbiol 33:721–731. https://doi.org/10.1046/j.1365-2958.1999.01519.x.
26. Muller CM, Conejero L, Spink N, Wand ME, Bancroft GJ, Titball RW. 2012. Role of RelA and SpoT in *Burkholderia pseudomallei* virulence and immunity. Infect Immun 80:3247–3255. https://doi.org/10.1128/IAI.00178-12.
27. Dean RE, Ireland PM, Jordan JE, Titball RW, Oyston PC. 2009. RelA regulates virulence and intracellular survival of *Francisella novicida*. Microbiology 155:4104–4113. https://doi.org/10.1099/mic.0.031021-0.
28. Haralalka S, Nandi S, Bhadra RK. 2003. Mutation in the *relA* gene of *Vibrio cholerae* affects *in vitro* and *in vivo* expression of virulence factors. J Bacteriol 185:4672–4682. https://doi.org/10.1128/JB.185.16.4672-4682.2003.
29. Sun W, Roland KL, Branger CG, Kuang X, Curtiss R, III. 2009. The role of relA and spoT in *Yersinia pestis* KIM5 pathogenicity. PLoS One 4:e6720. https://doi.org/10.1371/journal.pone.0006720.
30. Pizarro-Cerdá J, Tedin K. 2004. The bacterial signal molecule, ppGpp, regulates *Salmonella* virulence gene expression. Mol Microbiol 52:1827–1844. https://doi.org/10.1111/j.1365-2958.2004.04122.x.
31. Nakanishi N, Abe H, Ogura Y, Hayashi T, Tashiro K, Kuhara S, Sugimoto N, Tobe T. 2006. ppGpp with DksA controls gene expression in the locus of enterocyte effacement (LEE) pathogenicity island of enterohaemorrhagic *Escherichia coli* through activation of two virulence regulatory genes. Mol Microbiol 61:194–205. https://doi.org/10.1111/j.1365-2958.2006.05217.x.
32. Tapscott T, Kim J-S, Crawford MA, Fitzsimmons L, Liu L, Jones-Carson J, Vázquez-Torres A. 2018. Guanosine tetraphosphate relieves the negative regulation of *Salmonella* pathogenicity island-2 gene transcription exerted by the AT-rich *ssrA* discriminator region. Sci Rep 8:9465. https://doi.org/10.1038/s41598-018-27780-9.
33. Korch SB, Henderson TA, Hill TM. 2003. Characterization of the *hipA7* allele of *Escherichia coli* and evidence that high persistence is governed by (p)ppGpp synthesis. Mol Microbiol 50:1199–1213. https://doi.org/10.1046/j.1365-2958.2003.03779.x.
34. Fung DK, Chan EW, Chin ML, Chan RC. 2010. Delineation of a bacterial starvation stress response network which can mediate antibiotic tolerance development. Antimicrob Agents Chemother 54:1082–1093. https://doi.org/10.1128/AAC.01218-09.
35. Amato SM, Brynildsen MP. 2015. Persister heterogeneity arising from a single metabolic stress. Curr Biol 25:2090–2098. https://doi.org/10.1016/j.cub.2015.06.034.
36. Cohen NR, Lobritz MA, Collins JJ. 2013. Microbial persistence and the road to drug resistance. Cell Host Microbe 13:632–642. https://doi.org/10.1016/j.chom.2013.05.009.
37. Nguyen D, Joshi-Datar A, Lepine F, Bauerle E, Olakanmi O, Beer K, McKay G, Siehnel R, Schafhauser J, Wang Y, Britigan BE, Singh PK. 2011. Active starvation responses mediate antibiotic tolerance in biofilms and nutrient-limited bacteria. Science 334:982–986. https://doi.org/10.1126/science.1211037.
38. Betts JC, Lukey PT, Robb LC, McAdam RA, Duncan K. 2002. Evaluation of a nutrient starvation model of *Mycobacterium tuberculosis* persistence by gene and protein expression profiling. Mol Microbiol 43:717–731. https://doi.org/10.1046/j.1365-2958.2002.02779.x.
39. Dalebroux ZD, Svensson SL, Gaynor EC, Swanson MS. 2010. ppGpp conjures bacterial virulence. Microbiol Mol Biol Rev 74:171–199. https://doi.org/10.1128/MMBR.00046-09.
40. Dalebroux ZD, Swanson MS. 2012. ppGpp: magic beyond RNA polymerase. Nat Rev Microbiol 10:203–212. https://doi.org/10.1038/nrmicro2720.
41. Umland TC, Schultz LW, MacDonald U, Beanan JM, Olson R, Russo TA. 2012. *In vivo*-validated essential genes identified in *Acinetobacter baumannii* by using human ascites overlap poorly with essential genes detected on laboratory media. mBio 3:e00113-12. https://doi.org/10.1128/mBio.00113-12.
42. Sanchez-Larrayoz AF, Elhosseiny NM, Chevrette MG, Fu Y, Giunta P, Spallanzani RG, Ravi K, Pier GB, Lory S, Maira-Litrán T. 2017. Complexity of complement resistance factors expressed by *Acinetobacter baumannii* needed for survival in human serum. J Immunol 199:2803–2814. https://doi.org/10.4049/jimmunol.1700877.
43. Jung H-W, Kim K, Islam MM, Lee JC, Shin M. 12 February 2020. Role of ppGpp-regulated efflux genes in *Acinetobacter baumannii*. J Antimicrob Chemother https://doi.org/10.1093/jac/dkaa014.
44. Knight D, Dimitrova DD, Rudin SD, Bonomo RA, Rather PN. 2016. Mutations decreasing intrinsic beta-lactam resistance are linked to cell division in the nosocomial pathogen *Acinetobacter baumannii*. Antimicrob Agents Chemother 60:3751–3758. https://doi.org/10.1128/AAC.00361-16.
45. Brown DR, Barton G, Pan Z, Buck M, Wigneshweraraj S. 2014. Nitrogen stress response and stringent response are coupled in *Escherichia coli*. Nat Commun 5:4115. https://doi.org/10.1038/ncomms5115.
46. Clemmer KM, Bonomo RA, Rather PN. 2011. Genetic analysis of surface motility in *Acinetobacter baumannii*. Microbiology 157:2534–2544. https://doi.org/10.1099/mic.0.049791-0.
47. Skiebe E, de Berardinis V, Morczinek P, Kerrinnes T, Faber F, Lepka D, Hammer B, Zimmermann O, Ziesing S, Wichelhaus TA, Hunfeld KP, Borgmann S, Grobner S, Higgins PG, Seifert H, Busse HJ, Witte W, Pfeifer

Y, Wilharm G. 2012. Surface-associated motility, a common trait of clinical isolates of *Acinetobacter baumannii*, depends on 1,3-diaminopropane. Int J Med Microbiol 302:117–128. https://doi.org/10.1016/j.ijmm.2012.03.003.
48. Rumbo-Feal S, Perez A, Ramelot TA, Alvarez-Fraga L, Vallejo JA, Beceiro A, Ohneck EJ, Arivett BA, Merino M, Fiester SE, Kennedy MA, Actis LA, Bou G, Poza M. 2017. Contribution of the *A. baumannii* A1S_0114 gene to the interaction with eukaryotic cells and virulence. Front Cell Infect Microbiol 7:108. https://doi.org/10.3389/fcimb.2017.00108.
49. Eijkelkamp BA, Stroeher UH, Hassan KA, Elbourne LD, Paulsen IT, Brown MH. 2013. H-NS plays a role in expression of *Acinetobacter baumannii* virulence features. Infect Immun 81:2574–2583. https://doi.org/10.1128/IAI.00065-13.
50. Xiao H, Kalman M, Ikehara K, Zemel S, Glaser G, Cashel M. 1991. Residual guanosine 3′,5′-bispyrophosphate synthetic activity of *relA* null mutants can be eliminated by *spoT* null mutations. J Biol Chem 266:5980–5990.
51. Dahl JL, Arora K, Boshoff HI, Whiteford DC, Pacheco SA, Walsh OJ, Lau-Bonilla D, Davis WB, Garza AG. 2005. The *relA* homolog of *Mycobacterium smegmatis* affects cell appearance, viability, and gene expression. J Bacteriol 187:2439–2447. https://doi.org/10.1128/JB.187.7.2439-2447.2005.
52. Chatnaparat T, Li Z, Korban SS, Zhao Y. 2015. The bacterial alarmone (p)ppGpp is required for virulence and controls cell size and survival of *Pseudomonas syringae* on plants. Environ Microbiol 17:4253–4270. https://doi.org/10.1111/1462-2920.12744.
53. van Delden C, Comte R, Bally AM. 2001. Stringent response activates quorum sensing and modulates cell density-dependent gene expression in *Pseudomonas aeruginosa*. J Bacteriol 183:5376–5384. https://doi.org/10.1128/JB.183.18.5376-5384.2001.
54. Zhao G, Weatherspoon N, Kong W, Curtiss R, III, Shi Y. 2008. A dual-signal regulatory circuit activates transcription of a set of divergent operons in *Salmonella typhimurium*. Proc Natl Acad Sci U S A 105:20924–20929. https://doi.org/10.1073/pnas.0807071106.
55. Charity JC, Blalock LT, Costante-Hamm MM, Kasper DL, Dove SL. 2009. Small molecule control of virulence gene expression in *Francisella tularensis*. PLoS Pathog 5:e1000641. https://doi.org/10.1371/journal.ppat.1000641.
56. Fitzsimmons LF, Liu L, Kim J-S, Jones-Carson J, Vázquez-Torres A. 2018. *Salmonella* reprograms nucleotide metabolism in its adaptation to nitrosative stress. mBio 9:e00211-18. https://doi.org/10.1128/mBio.00211-18.
57. Cashel M. 1974. Preparation of guanosine tetraphosphate (ppGpp) and guanosine pentaphosphate (pppGpp) from *Escherichia coli* ribosomes. Anal Biochem 57:100–107. https://doi.org/10.1016/0003-2697(74)90056-6.
58. Neidhardt FC, Bloch PL, Smith DF. 1974. Culture medium for enterobacteria. J Bacteriol 119:736–747. https://doi.org/10.1128/JB.119.3.736-747.1974.
59. Ducas-Mowchun K, De Silva PM, Crisostomo L, Fernando DM, Chao T-C, Pelka P, Schweizer HP, Kumar A. 2019. Next generation of Tn*7*-based single-copy insertion elements for use in multi- and pan-drug-resistant strains of *Acinetobacter baumannii*. Appl Environ Microbiol 85:e00066-19. https://doi.org/10.1128/AEM.00066-19.
60. Wachino J-I, Jin W, Kimura K, Arakawa Y. 2019. Intercellular transfer of chromosomal antimicrobial resistance genes between *Acinetobacter baumannii* strains mediated by prophages. Antimicrob Agents Chemother 63:e00334-19. https://doi.org/10.1128/AAC.00334-19.
61. Farinha MA, Kropinski AM. 1990. Construction of broad-host-range plasmid vectors for easy visible selection and analysis of promoters. J Bacteriol 172:3496–3499. https://doi.org/10.1128/JB.172.6.3496-3499.1990.
62. Hunger M, Schmucker R, Kishan V, Hillen W. 1990. Analysis and nucleotide sequence of an origin of DNA replication in *Acinetobacter calcoaceticus* and its use for *Escherichia coli* shuttle plasmids. Gene 87:45–51. https://doi.org/10.1016/0378-1119(90)90494-C.
63. Schmittgen TD, Livak KJ. 2008. Analyzing real-time PCR data by the comparative *CT* method. Nat Protoc 3:1101–1108. https://doi.org/10.1038/nprot.2008.73.